

# Electron transfer in pristine and functionalised single-walled carbon nanotubes

Matteo Iurlo, Demis Paolucci, Massimo Marcaccio and Francesco Paolucci\*

Received (in Cambridge, UK) 2nd June 2008, Accepted 2nd July 2008

First published as an Advance Article on the web 21st August 2008

DOI: 10.1039/b809285k

Since their very first days, electron transfer has always played a special role in carbon nanotubes' life. In view of their structural and electronic uniqueness, carbon nanotubes have been proposed either as bulk electrode materials for sensing and biosensing in advanced electrochemical devices, or as molecular-sized electrodes for very fast electrode kinetics investigations. Alternatively, electron transfer has been used to probe the electronic properties of carbon nanotubes by either direct voltammetric inspection or coupling with spectroscopic techniques, ultimately allowing, in the case of true solutions of individual uncut single-walled carbon nanotubes (SWNTs), to single-out their redox potentials as a function of diameter. For their redox properties, as emerged from these studies, SWNTs represent unique building blocks for the construction of photofunctional nanosystems to be used in efficient light energy conversion devices.

## Introduction

Carbon nanotubes (CNTs) show unique features that are proposed for the development of nanometer scale materials with outstanding potential technological applications,<sup>1</sup> in a process that is accompanied by a constantly increasing understanding of many of their properties. Issues that may greatly hamper their widespread technological use comprise the difficult processibility of SWNTs in liquid phases and the currently unavoidable structural heterogeneity of as-synthesized SWNTs, and are now being overcome.<sup>2</sup> Most common processing procedures involve dispersing the nanotubes either by the help of a dispersant phase, a surfactant,<sup>3</sup> a biomolecule,<sup>4</sup> or a polymer,<sup>5</sup> by dilution<sup>6</sup> or by chemical covalent or non-covalent functionalisation,<sup>7</sup> reduction<sup>8</sup> or protonation by superacids.<sup>9</sup> Aqueous micelle-like suspensions of individual

SWNTs recently opened the door to powerful experimental approaches for extracting optical properties through bulk measurements.<sup>10</sup> Beside the already existing commercial uses of nanotubes,<sup>11a</sup> feasible nanotube applications for the near and long term comprise electronic devices and interconnects, field emission devices, electrochemical devices, sensors and biosensors, electromechanical actuators, polymer composites, and drug-delivery systems.<sup>11</sup>

A single-walled carbon nanotube (SWNT) is often described as the result of seamless wrapping of a graphene sheet into a cylinder along the  $(n,m)$  roll-up vector. The  $(n,m)$  indices fully define the SWNT radius and chirality and determine unequivocally its electronic structure (Scheme 1).<sup>12</sup> If  $|n - m| = 3q$ , where  $q$  is an integer, the SWNT is metallic, whereas for  $|n - m| \neq 3q$  it is semiconducting with a band gap in the density of states (DOS) whose size is inversely proportional to the diameter. As a consequence of the size-dependent quantization of electronic wave functions around the circumference of the SWNT, the DOS shows typical singularities, the so-called van Hove singularities, consisting of a singular

*INSTM, Unit of Bologna, Dipartimento di Chimica, Università di Bologna, Via Selmi 2, I-40126 Bologna, Italy.*

*E-mail: francesco.paolucci@unibo.it; Fax: 39 051 2099456;*

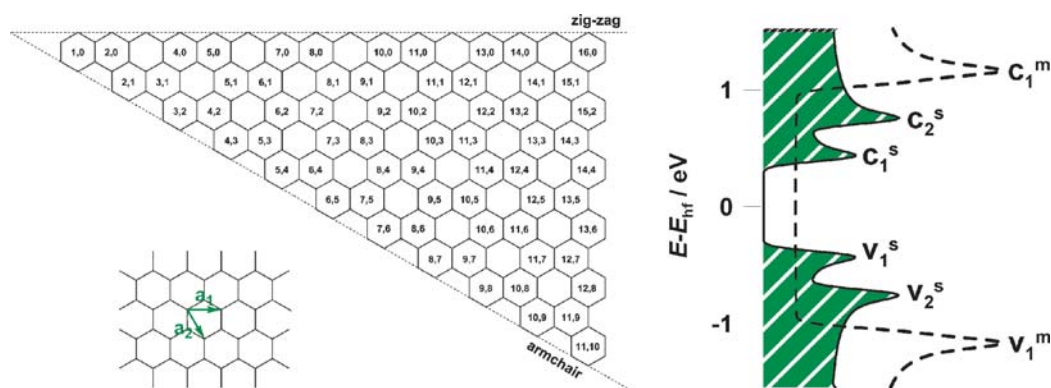
*Tel: 39 051 2099460*

*Matteo Iurlo received his Laurea degree in Chemistry in 2006 from the University of Bologna and is currently a PhD student at the Department of Chemistry "G. Ciamician" in Paolucci's group. His research interests focus on physical chemical characterization and manipulation of carbon nanotubes by using electrochemical and spectroelectrochemical techniques in solution and on surfaces.*

*Demis Paolucci received his PhD in supramolecular electrochemistry and nanotechnology, under Prof. Paolucci. He has also spent research periods at the Universities of Bristol, Nottingham and Montpellier. His research work deals mainly with the electrochemical investigation of organised supramolecular and biologically-active systems as functional materials for technological applications, fullerene and carbon nanotubes.*

*Massimo Marcaccio is an Assistant Professor at the University of Bologna. His main research interests concern the electrochemical and spectroelectrochemical investigation of a variety of molecular and supramolecular systems, metal transition coordination species, fullerenes, corannulene, carbon nanotubes and proteins and, most recently, electrochemiluminescence and scanning probe microscopy techniques.*

*Francesco Paolucci is an Associate Professor at the University of Bologna. His research interests include electrochemically-induced reactions involving metal complexes, mechanically-interlocked systems, fullerenes and carbon nanotubes, biologically-active systems and, most recently, electrochemiluminescence and scanning probe electrochemical microscopy.*



**Scheme 1** Left: each pair of indexes  $(n,m)$  defines the length and chiral angle of the SWNT roll-up vector ( $\pi$  times the tube diameter) on a graphene sheet. Structures having  $|n - m| \neq 3q$  ( $q = \text{integer}$ ) are only shown in the chirality map, that correspond to semiconducting nanotubes. Right: qualitative pattern of van Hove peaks for a semiconducting (green) or a metallic (dashed line) SWNT

increase in the DOS at energies  $\varepsilon_{\text{vH}}$  followed by a  $(\varepsilon - \varepsilon_{\text{vH}})^{-1/2}$  decrease (Scheme 1).

About one third of all the SWNTs are metallic and always have wider energy gaps between the first van Hove singularities than semiconducting ones with similar diameter. The presence of the van Hove singularities dominates the spectral features of these species<sup>13</sup> and, as we shall see below, also the electrochemical ones.

### Electronic properties vs. electrochemistry of SWNTs

The electronic properties of a SWNT are unequivocally determined by its diameter and helicity, although some additional quantum confinement was recently shown in ultrashort SWNTs.<sup>14</sup> In turn, their optical properties are dominated by the electronic transition between pairs of van Hove singularities, that, in neutral nanotubes, are symmetrically located on either side of the Fermi level. Such intragap transitions, denoted  $S_{11}$ ,  $S_{22}$ , *etc.* (for semiconducting SWNTs) or  $M_{11}$ , *etc.* (for metallic ones), according to which pair of van Hove singularities are involved, are obviously important for absorption and emission electronic spectroscopic investigations and also play an important role in resonance-Raman spectroscopy because they greatly enhance the Raman intensity. Recently, the mapping of each optical transition to a specific  $(n,m)$  structure in HiPco samples was achieved through a combination of intragap fluorescence spectroscopy and resonance Raman data in surfactant-stabilized aqueous suspensions of SWNTs.<sup>15</sup> On the other hand, when SWNTs undergo either n- or p-doping, their intragap transitions (both absorption and emission) and the Raman radial breathing modes are largely bleached and such a behaviour was then used to obtain information relative to the redox properties of SWNTs.<sup>16</sup> It is assumed that p- and n-doping causes depletion of the valence band and the filling of the conduction band in SWNT, respectively. These changes in electron density would then lead to bleaching of the electronic transition between van Hove singularities in the visible and near-infrared regions and produce decreases in resonant-Raman intensity.

Chemical doping of SWNTs<sup>17</sup> was obtained by charge-transfer reactions with either electron donors (*e.g.* alkali metals<sup>15,16</sup> and anion radicals<sup>15,18</sup>) or acceptors (*e.g.* halides,<sup>15</sup>

organic acceptors<sup>19</sup> and oxygen<sup>20</sup>) and was used to produce sizeable changes in either the absorption Vis-NIR or Raman spectra of SWNTs. The energies of the LUMOs relative to the vacuum level of a range of semiconducting SWNTs were recently determined using a biohybrid approach and Nernst equation.<sup>21</sup> Electrochemical control of the *reducing/oxidising strength* allows, on the other hand, a much finer control of the doping level in the SWNTs and was indeed largely used, coupled to either absorption Vis-NIR or Raman spectroscopy, as reported in a series of publications in years 2000–2007 that were very recently reviewed.<sup>22</sup> In most cases such studies have mainly been confined to immobilised systems where the SWNTs were either spin-coated or drop-cast onto conductive supports or otherwise narrowly packed in self-standing bucky paper. Thus, the strong tube–tube and tube–substrate interactions gave poorly resolved spectra, without proper matching of specific optical transitions to individual SWNTs. Raman scattering of isolated SWNTs on gold surfaces in aqueous solution was also investigated under electrochemical control,<sup>23</sup> and the spectral changes induced by electrochemical doping were correlated to the difference in electronic density of individual SWNT with distinct diameter and chirality.

### Electrochemistry at carbon nanotubes

Carbon is commonly used as electrode material for electrochemistry;  $\text{sp}^2$  carbon, in particular, combines a wide useful potential window with electronic properties similar to metals.<sup>24</sup> Additionally, chemical surface modification of carbon is an important viable approach to functional electrodes.<sup>25</sup> Covalent grafting of organic monolayers on carbon (graphite, HOPG, carbon fibers, *etc.*) can be obtained by the electrochemical *in situ* reduction of aryl diazonium salts or the oxidation of aromatic and/or aliphatic amines. Such electrochemical methods produce a monolayer of an organic species through the formation of a carbon–carbon (or carbon–nitrogen) bond between the carbon surface and the functionalizing compound.<sup>25</sup> Carbon nanotubes represent a new kind of carbon materials that are superior to other kinds of carbon materials such as glassy carbon, graphite and diamond. For their special structural features and unique electronic properties, NTs have found applications in electrocatalysis, direct

electrochemistry of proteins and electroanalytical devices, such as electrochemical sensors and biosensors. The electroanalytical applications of carbon nanotubes have been thoroughly described in a series of recent reviews.<sup>26</sup>

Recently, there has been a large interest in using SWNTs as electrodes for electrochemistry stemming from the prospect of using individual SWNTs as carbon nanoelectrodes or ensembles of SWNTs as large surface-area carbon electrodes.<sup>26</sup> Individual SWNTs can be used as nanoelectrodes for electrochemistry, yielding enhanced mass transport and high current densities equivalent to sub-10 nm hemispherical electrodes, thus giving access to very fast electrode kinetics such as the oxidation of ferrocenes.<sup>27</sup>

The interesting, unconventional electronic properties relating to SWNTs also deserved some special electrochemical theoretical treatment. The heterogeneous electron transfer kinetics to SWNTs was recently modelled through a combination of electrochemical gating and electrochemical charge transfer by applying the Gerischer–Marcus model.<sup>28</sup> The model showed that interfacial capacitances have a large impact on the behavior of electron transfer at SWNT electrodes since a potential applied between an SWNT and the electrolyte can very effectively change the chemical potential of the SWNT.

## Electrochemistry of carbon nanotubes

The close proximity of the substrate and/or the intra-bundle (inter-tube) interactions may have large effects on their electronic properties.<sup>29</sup> A way to minimise such interactions and thus obtain valuable information concerning the redox (electronic) properties of non-interacting individual NTs, complementary to those given by spectroscopy, is to carry out electrochemical investigations in suitable solutions of *individual* NTs. Among the reasons why this approach has so far found much more limited applications *vis-à-vis* spectroscopic methods are (i) the relatively lower sensitivity of electrochemical techniques with respect to spectroscopic ones, (ii) the interference in the electrochemical measurements from most of the molecular systems (surfactants, polymer chains, DNA) used for making SWNT suspensions, (iii) the high ionic strength typical of electrochemical experiments (due to the addition of a supporting electrolyte) that promotes flocculation of the SWNT suspension and (iv) the limited electrochemical stability window of the aqueous medium.

### Cyclic voltammetric investigations of solutions of individual SWNTs

We recently reported on the voltammetric behaviour of (N-TEG)-pyrrolidine functionalised SWNTs (*f*-NT) in tetrahydrofuran solutions (Fig. 1).<sup>30</sup> A combination of electrochemical measurements and quantum chemical calculations was made in order to address two major issues with *f*-NT, *i.e.*, the nature of their bulk electronic properties, and to what extent they retain those of pristine NT. The steady-state voltammetric curve obtained at an ultramicroelectrode (UME) displays a continuum of diffusion-controlled current, with onset, in the negative potential region, at  $\sim -0.5$  V, which is attributed to the reduction of *f*-NTs.

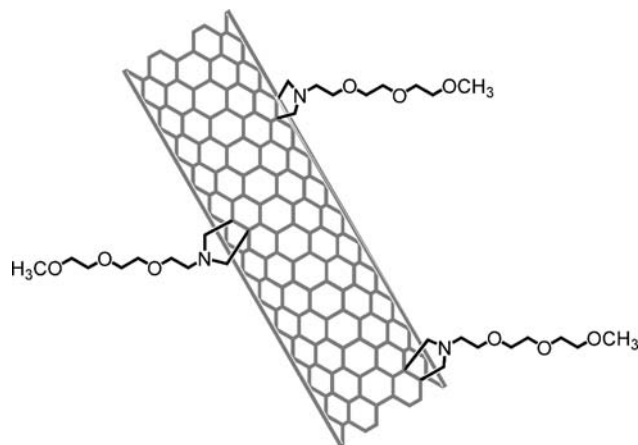


Fig. 1 N-TEG pyrrolidine-SWNT.

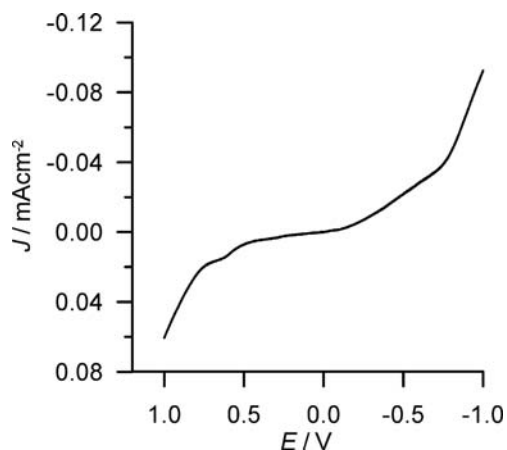


Fig. 2 Steady-state CV curve of saturated *f*-NTs, 0.01 M TBAH, THF solution:  $\nu = 0.5$  V s,  $T = 25$  °C at a Au electrode derivatized with a dodecanethiol self-assembled monolayer. Potentials measured vs. silver quasi-reference electrode.

Experiments were carried out with a gold UME modified by a self-assembled monolayer of dodecanethiols, according to a procedure proposed by Becka and Miller<sup>31</sup> (Fig. 2). The presence of the organic monolayer slows down the heterogeneous electron transfer process, thus avoiding competition from diffusion. The measured current thus becomes representative of the SWNTs DOS and could therefore be compared with that calculated for pristine SWNTs from the electronic density of states, according to a simple equation (eqn (1)).<sup>32</sup>

$$i(E_f) \propto \int_0^{E_f} (\text{DOS}) dE \quad (1)$$

The DOS of pristine SWNTs was calculated according to a tight binding model<sup>33</sup> and averaged over 39 different NTs with diameters between 0.88 and 1.22 nm and relative abundances that correspond to the population of tubes contained in HiPCO samples probed in the voltammetric experiments.<sup>34</sup>

The comparison showed that the overall DOS is not strongly affected by the chemical modification. However, the

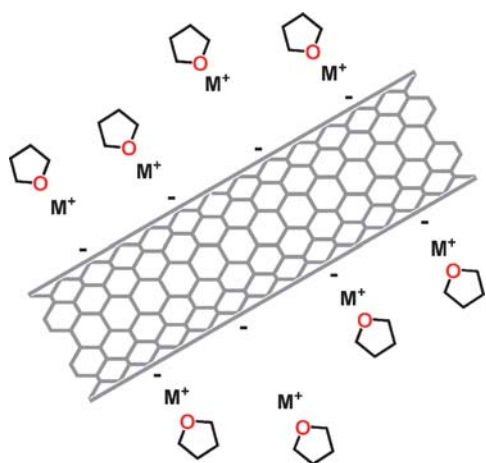


**Fig. 3** Schematic structure of the soluble SWNTs salts  $M^+(THF)_n$  ( $M^+ = Na^+, K^+$ ).

DOS of  $f$ -NT shows a smoothing of the peaks that appear in pristine NT at about  $\pm 0.5$  eV. Such peaks are related to the van Hove singularities between which electronic transitions take place and in fact, experimentally, this class of  $f$ -NT shows a rather flat near-infrared spectrum.

Proper *solution* electrochemical experiments on pristine SWNTs were only possible after the recent discovery of an innovative way to form thermodynamically stable solutions of unmodified and uncut SWNTs.<sup>8</sup> Upon reduction with alkali metals, SWNTs produce polyelectrolyte salts (Fig. 3) that are soluble in polar organic solvents without use of sonication, surfactants, or functionalization. Polyelectrolyte SWNT salts were obtained by reacting arc-discharge samples ( $a$ -NT) or HiPco samples ( $h$ -NT) with different alkali metals (Na, K).<sup>8</sup>

Voltammetric experiments were carried out in oxygen free, ultra-dry DMSO where, to avoid flocculation of the SWNTs, only low concentrations of the supporting electrolyte were used.<sup>35</sup> Fig. 4 compares the voltammetric curves of a saturated

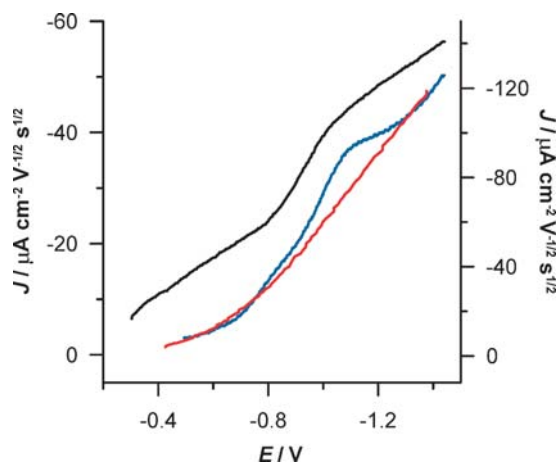


**Fig. 4** CV curves of DMSO solutions saturated with Na[ $a$ -NT] (black line), saturated Na[ $h$ -NT] (blue line) or saturated  $f$ -NT (red line). The black and blue curves are referred to the left axis, the red curve to the right axis. Experimental conditions: 2 mM TBAH–DMSO; working electrode: Pt disk ( $r = 25 \mu\text{m}$ );  $T = 298$  K; scan rate  $1 \text{ V s}^{-1}$ . Potentials are referenced to SCE.

DMSO solution of Na[ $a$ -NT] and Na[ $h$ -NT] with that of  $f$ -NT, at potentials close to the open circuit potential (OCP). The curves show that: (i) the potential where the current onset occurs is less negative for Na[ $a$ -NT] with respect to Na[ $h$ -NT] and  $f$ -NT (that were also produced from HiPco SWNTs); (ii) the curves of  $h$ -NT and  $a$ -NT (for both  $K^+$  and  $Na^+$  salts) are richer in structure than that of  $f$ -NT. In particular, the broad waves at  $-0.81$  and  $-1.05$  V ( $h$ -NT) and  $-0.56$  and  $-0.99$  V ( $a$ -NT) are missing for  $f$ -NT.

The lower potential for the current onset is indicative of a smaller energy gap, consistent with the larger average diameters of the arc-SWNTs with respect to the HiPco ones. The richer curve morphology reflects, instead, the more complex electronic structure of the pristine materials, compared with  $f$ -NT, thus confirming that functionalization significantly affects the low lying electronic states of the nanotubes.

### Vis-NIR spectroelectrochemical investigation of true solutions of unfunctionalized SWNTs

The voltammetric response of individual SWNTs in solution reflects average collective properties rather than single SWNT

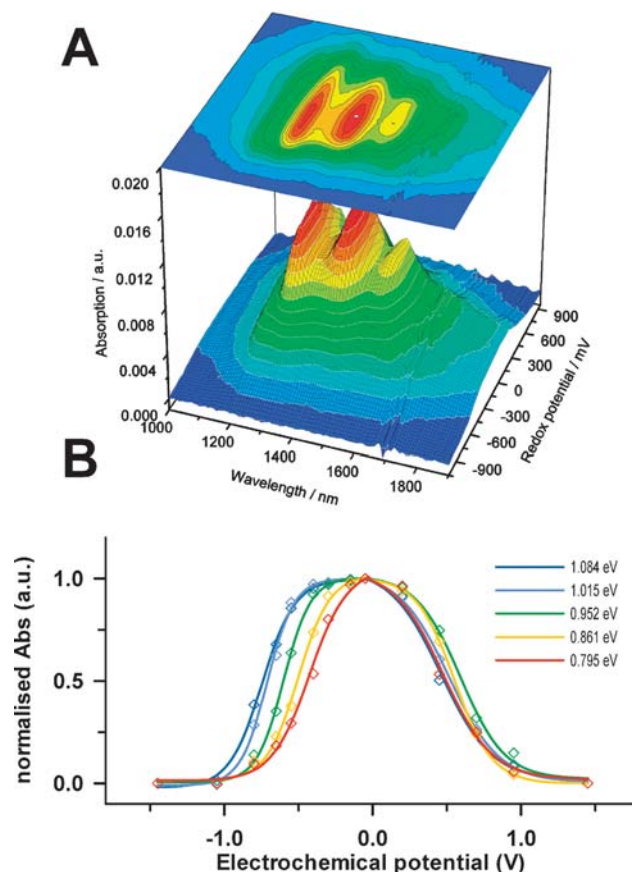


**Fig. 5** (a) Smoothed surface plot of optical absorption intensity as a function of wavelength and electrode potential in the  $S_{11}$  region for K[ $h$ -NT]. (b) Intensity of each of the five bands selected in the spectra above after normalization as a function of potential. The fitting curves (full lines) were calculated using eqn (2), whence  $E_{ox,i}^0$  and  $E_{red,i}^0$  values were obtained (corresponding to the inflection points in each sigmoidal curve). In all plots raw electrochemical data, *i.e.* uncorrected for ohmic drop, are referenced to SCE.

ones and is not therefore a suitable technique to determine the standard redox potentials of individual semiconducting SWNTs as a function of the tube structure. This was instead achieved *via* an extensive Vis-NIR spectroelectrochemical investigation of true solutions of polyelectrolyte SWNT solutions that was carried out in the  $\pm 1500$  mV range (*vs.* SCE) where doping is expected to modify the population of the first and second van Hove singularities of the electronic bands of SWNTs. The electronic transitions affected by charging are therefore the semiconducting  $S_{11}$  ( $v_s^1 \rightarrow c_s^1$ ) and  $S_{22}$  ( $v_s^2 \rightarrow c_s^2$ ) and possibly the metallic  $M_{11}$  ( $v_m^1 \rightarrow c_m^1$ ).<sup>13</sup>

As expected for heavily n-doped SWNTs, the starting solutions do not show significant absorption except for the plasmon band, typical of graphitic materials.<sup>7b,16</sup> Spectral changes were recorded as long as the applied potential was increased above  $-1.2$  V, associated with the progressive undoping of SWNTs: the intensity increased progressively until the maximum was reached for the complete depletion of the conduction bands.

The 3D plot of Fig. 5(A) displays a summary of the spectroelectrochemical investigation of the *h*-NT  $S_{11}$  region. On both reduction and oxidation sides, the absorption bands have different onset potentials thus suggesting that different redox potentials are associated to different tube structures.

### Standard redox potentials of individual SWNTs in solution

The knowledge of the oxidation and reduction potentials of SWNTs is instrumental to the rational design of electrochemical, photochemical and electronic devices, such as sensors, photoactive dyads, light emitting diodes or other electroluminescent devices, in which the energetics of electrochemical and electric generation of electrons and holes in the SWNTs play an important role. The analysis of the spectroelectrochemical results of *h*-NT and *a*-NT shown above allowed to obtain the standard redox potential as a function of the tube diameter of a large number of semiconducting SWNTs. In the analysis, we assumed that the absorbance is due only to neutral SWNTs (and according to the Lambert–Beer law), and that the Nernst equation describes the ratios of activity (concentration) of the neutral-to-reduced (or -oxidized) SWNTs. Therefore, the absorbance ( $A$ ) of the samples is described as a function of electrochemical potential by two equations (eqn (2)) for the n- and p-doped SWNTs, respectively:<sup>36</sup>

$$A_{n\text{-dop},i} = \varepsilon_{N,i} b c_i^* \frac{e^{\frac{F}{RT}(E - E_{\text{red},i}^0)}}{1 + e^{\frac{F}{RT}(E - E_{\text{red},i}^0)}} \quad (2a)$$

$$A_{p\text{-dop},i} = \varepsilon_{N,i} b c_i^* \frac{1}{1 + e^{\frac{F}{RT}(E - E_{\text{ox},i}^0)}} \quad (2b)$$

where  $i$  is a single ( $n,m$ ) nanotube that contributes to a specific transition band,  $\varepsilon_N$  is the extinction coefficient of the neutral ( $n,m$ ) nanotube (for simplicity assumed to be the same for all tubes),  $c^*$  is its bulk concentration,  $E$  is the electrochemical potential,  $b$  is the path of the spectroscopic cell, and  $E_{\text{red},i}^0$  and  $E_{\text{ox},i}^0$  are the standard potentials of its reduction (n-doping) and oxidation (p-doping). After normalization (Fig. 5(B)), the intensity of each band in the spectra was analyzed according to eqn (2), to give a set of standard potentials for the oxidations and reductions of *h*-

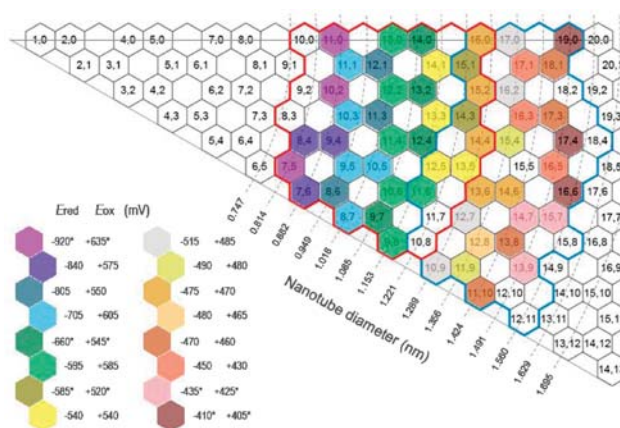


**Fig. 6** Chirality map displaying the average standard potentials associated to SWNT structures typically present in commercial samples. HiPco SWNTs are located inside the red line, while arc-discharge SWNTs are inside the blue line.

NT and *a*-NT. The assignment of the redox potentials were obtained by adopting the empirical Kataura plot of ref. 37 which give the excitation energies of the van Hove optical transitions as a function of the structure for a wide range of semiconducting nanotubes. Finally, the  $E^0$ 's vary linearly with the excitation energy: to first order, the redox potential fit the equations:

$$E_{\text{red}}^0 = -1.02E_{\text{exc}} + 0.26 \quad (R^2 = 0.989) \quad (3a)$$

$$E_{\text{ox}}^0 = 0.36E_{\text{exc}} + 0.22 \quad (R^2 = 0.704) \quad (3b)$$

that can be employed in the design of devices mentioned above. The chirality map of Fig. 6, where color codes are used to gather the structures that share the same values, shows that, in analogy with optical transition frequencies, a simple dependence of redox properties of SWNTs on diameter is not strictly followed.

### Fermi level and excitonic binding energy of the nanotubes from electrochemical data

The energy of the Fermi level in the neutral state ( $E_f$ ) calculated from the standard redox potentials, is almost constant for *a*-NTs, while for *h*-NTs it is linear with the energy of the optical gap.<sup>35</sup> The trend is in line with other reported experimental values and is also reproduced by *ab initio* calculations. Furthermore, standard redox potentials were finally used to establish the exciton binding energy for individual tubes in solution. For each SWNT, the difference of the redox potentials represents the gap between the van Hove singularities of the electronic band structure ( $E_{\text{gap}} = E_{\text{ox}} - E_{\text{red}}$ ).  $E_{\text{gap}}$  is larger than the excitation energy because of the Coulomb attraction experienced by the excited electron with the positive hole left in the valence band,  $E_{\text{exc}} < E_{\text{gap}}$ .<sup>38</sup> The excitonic binding energy calculated from the electrochemical data given by eqn (3) is inversely proportional to the nanotube diameter and matched very well the excitonic binding energies obtained elsewhere.

### Photoinduced electron transfer in donor–acceptor ensembles

Carbon nanotubes possessing electroactive, photoactive, catalytic and biologically active functional components

coupled to their surface with useful potential applications in medicine,<sup>11c</sup> sensors and biosensors<sup>25,39</sup> and light-energy harvesting devices<sup>40</sup> are a topic of great research interest. The presence of extended, delocalized  $\pi$ -electron systems renders most CNTs very useful for managing charge transfer and charge transport. In this respect, CNTs have been mostly considered, in analogy to fullerenes, as good electron acceptors, with the additional property of quasi-ballistic electron transport along their tubular axis.<sup>41</sup> Advances in the use of CNTs in photovoltaic devices for photocurrent generation have been very recently reviewed.<sup>42</sup>

Following our recent report on the first intramolecular electron transfer within a photoexcited SWNT and ferrocene moieties covalently linked to it<sup>43</sup> (structure **1** in Fig. 7), a large number of photoactive dyads based on SWNTs have been reported,<sup>44</sup> a small collection of which is shown in Fig. 7 and 8 (structures **1–4**). In such dyads, the electron donors—mostly ferrocenyl derivatives, extended-TTF, porphyrinoid and metalloporphyrinoid systems—have been electronically coupled to the SWNT surface either by covalent attachment onto the sidewalls of SWNTs or, alternatively, by supramolecular van der Waals/electrostatic interactions. Hydrogen bonding, complementary electrostatics,  $\pi$ - $\pi$  stacking and metal coordination, giving rise to many diverse hybrid systems in which the hierarchical integration of multiple components into well-ordered arrays allows to achieve highly efficient vectorial *intra-ensemble* charge transfer processes.<sup>44</sup> Typically, intramolecular electron transfer processes within these nano-hybrids were probed by fluorescence and transient absorption spectroscopy,<sup>45</sup> while electrochemical techniques, mainly

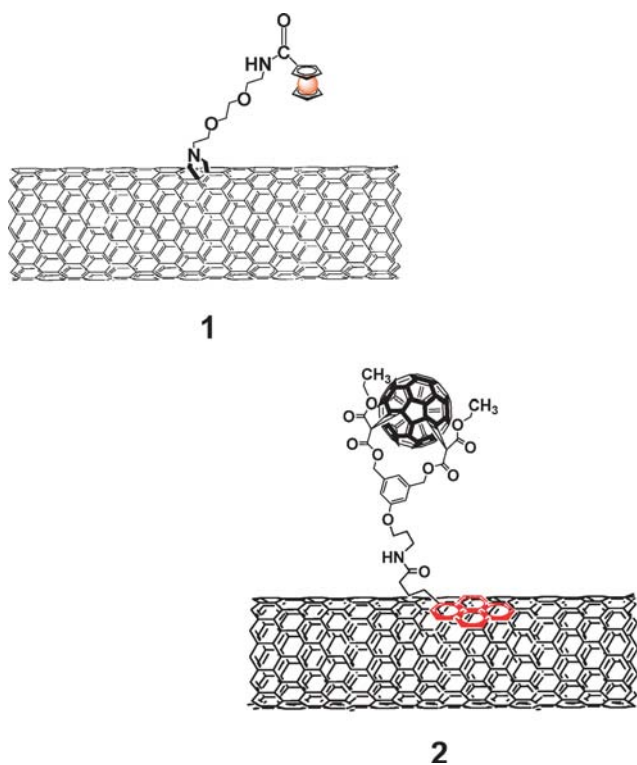


**Fig. 7** First examples of covalently-linked photoactive dyads (**1**) and supramolecular hybrid C<sub>60</sub>-pyrene-SWNT (**2**).

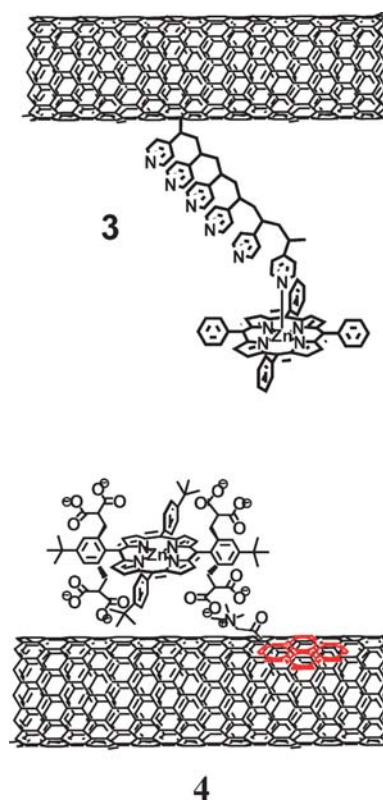


**Fig. 8** Photoactive dyads: different strategies for coupling of SWNTs to a Zn-porphyrin.

voltammetry and spectroelectrochemistry, were used to monitor the sizeable electronic interaction between donor and acceptor moieties in the ground state.

As mentioned above, in the majority of these studies, the SWNTs acted as electron acceptors. However, as shown in Fig. 6, SWNTs present much lower oxidation potentials than C<sub>60</sub>,<sup>46</sup> thus making them, at variance with the latter, suitable for their alternative use as electron donors. In fact, supramolecular nano-hybrids composed of single-wall carbon nanotubes and fullerene derivatives were constructed and studied. A C<sub>60</sub>-bisadduct bearing a pyrene unit was used to solubilize the SWNTs and the resulting nano-hybrid (structure **2** in Fig. 7) was investigated by cyclic voltammetry, transmission electron microscopy, and photophysical experiments that confirmed the existence of  $\pi$ - $\pi$  interactions and intra-hybrid photoinduced charge transfer processes responsible for the quenching of fullerene emission.<sup>47</sup> A similar supramolecular approach, in which both  $\pi$ - $\pi$  stacking of pyrene on the SWNT surface, and alkyl ammonium-crown ether interactions were used in the self-assembly process of a fullerene derivative with SWNTs, was recently reported.<sup>48</sup> The nano-hybrid integrity was probed with various spectroscopic techniques, TEM and electrochemical measurements. Nanosecond transient absorption studies confirmed electron transfer as the quenching mechanism of the singlet excited-state of C<sub>60</sub> in the nano-hybrid resulting into the formation of SWNT<sup>+</sup>/Pyr-NH<sub>3</sub><sup>+</sup>/crown-C<sub>60</sub>-charge-separated state.

Recently, other carbon nanostructures, such as carbon nanohorns (CNHs), have been integrated with photoactive

electron donors, such as porphyrins and pyrenes. CNHs are characterised by a very high purity and possess a unique morphology comprising a secondary superstructure forming physically inseparable spherical aggregates and are currently under intense investigation for practical technological applications such as photochemical water splitting and as catalysts for the reduction of CO<sub>2</sub> to fuels. We recently described the functionalization of carbon nanohorns and the creation of new SWNH/porphyrin nanoconjugates.<sup>49</sup> The electrochemical experiments revealed sizeable electronic interactions of porphyrins with SWNHs in the nanoconjugate. Transient absorption spectra permitted to highlight electron transfer process between the porphyrins and the carbon nanostructures.

New metallo-nanostructured materials of carbon nanohorns were recently prepared by the coordination of Cu(II)-2,2':6',2''-terpyridine (Cu<sup>II</sup>tpy) with oxidized carbon nanohorns (CNHs-COOH) and the resulting CNHs-COO-Cu<sup>II</sup>tpy metallo-nanocomplexes have shown efficient fluorescence quenching, suggesting that electron transfer occurs from the singlet excited state of Cu<sup>II</sup>tpy to CNHs.<sup>50</sup>

## Conclusions and perspectives

Carbon is unique in nature. Beside its capability to form complex networks that is fundamental to organic chemistry, elemental carbon also shows unrivalled complexity among the elements, forming many allotropes, from 3D diamond and graphite to 0D fullerenes, through 1D nanotubes and the most recently obtained 2D graphene.<sup>51</sup> Over the last two decades we have assisted to the subsequent rise of the three different low-dimensional carbon allotropes. After being the chemists' superstar in the 1990s, C<sub>60</sub> is still at the centre of considerable attention in many different fields of science.<sup>52</sup>

Carbon nanotubes are perhaps the most notable representatives of the present nanoworld. However, they are very likely bound to share soon the stage with graphene, the "rapidly rising star on the horizon of materials science and condensed-matter physics".<sup>53</sup> Graphene consists of a two-dimensional hexagonal lattice of sp<sup>2</sup> carbon, through which electronic conduction can occur *via* the  $\pi$ -conjugated electron system, and is sometimes classified as a zero-gap semiconductor, since the density of states per unit area vanishes at the Fermi level.

The unique properties predicted for graphene comprise a number of very unusual electronic properties—from an anomalous quantum Hall effect to the absence of localization. As new procedures for the large-scale production of graphene are expected to be developed in the near future, most of such properties—and those still unknown—will be soon experimentally demonstrated, thus permitting the development of the many important technological applications foreseen for this material.

## Acknowledgements

This work was performed with partial support from the University of Bologna, the Fondazione Cassa di Risparmio in Bologna and the Italian Ministry of University and Research.

## Notes and references

- R. H. Baughman, A. A. Zakhidov and W. A. de Heer, *Science*, 2002, **297**, 787–792.
- (a) N. Grobert, *Mater. Today*, 2007, **10**(1–2), 28–35; (b) M. S. Arnold, A. A. Green, J. F. Hulvat, S. I. Stupp and M. C. Hersam, *Nat. Nanotechnol.*, 2006, **1**, 60–65; (c) L. Zhang, S. Zaric, X. M. Tu, X. R. Wang, W. Zhao and H. J. Dai, *J. Am. Chem. Soc.*, 2008, **130**, 2686–2691; (d) S.-Y. Ju, J. Doll, I. Sharma and F. Papadimitrakopoulos, *Nat. Nanotechnol.*, 2008, **3**, 356–362.
- G. S. Duesberg, M. Burghard, J. Muster, G. Philipp and S. Roth, *Chem. Commun.*, 1998, 435–436.
- M. Zheng, A. Jagota, E. D. Semke, B. A. Diner, R. S. McLean, S. R. Lustig, R. E. Richardson and N. G. Tassi, *Nat. Mater.*, 2003, **2**, 338–342.
- (a) A. Nish, J.-Y. Hwang, J. Doig, R and J. Nicholas, *Nat. Nanotechnol.*, 2007, **2**, 640–646; (b) R. Murphy, J. N. Coleman, M. Cadek, B. McCarthy, M. Bent, A. Drury, R. C. Barklie and W. J. Blau, *J. Phys. Chem. B*, 2002, **106**, 3087–3091.
- (a) S. Giordani, S. D. Bergin, V. Nicolosi, S. Lebedkin, M. K. Kappes, W. J. Blau and J. N. Coleman, *J. Phys. Chem. B*, 2006, **110**, 15708–15718; (b) S. D. Bergin, V. Nicolosi, P. V. Streich, S. Giordani, Z. Sun, A. H. Windle, P. Ryan, N. P. P. Niraj, Z.-T. T. Wang, L. Carpenter, W. J. Blau, J. J. Boland, J. P. Hamilton and J. N. Coleman, *Adv. Mater.*, 2008, **20**, 1–6.
- (a) S. Banerjee, T. Hemraj-Benny and S. S. Wong, *Adv. Mater.*, 2005, **17**, 17–29; (b) S. Niyogi, M. A. Hamon, H. Hu, B. Zhao, P. Bhowmik, R. Sen, M. E. Itkis and R. C. Haddon, *Acc. Chem. Res.*, 2002, **35**, 1105–1113; (c) Q. Xiao, P. H. Wang and Z. C. Si, *Prog. Chem.*, 2007, **19**, 101–106.
- A. Penicaud, P. Poulin, A. Derre, E. Anglaret and P. Petit, *J. Am. Chem. Soc.*, 2005, **127**, 8–9.
- S. Ramesh, L. M. Ericson, V. A. Davis, R. K. Saini, C. Kittrell, M. Pasquali, W. E. Billups, W. W. Adams, R. H. Hauge and R. E. Smalley, *J. Phys. Chem. B*, 2004, **108**, 8794–8798.
- M. J. O'Connell, S. M. Bachilo, C. B. Huffman, V. C. Moore, M. S. Strano, E. H. Haroz, K. L. Rialon, P. J. Boul, W. H. Noon, C. Kittrell, J. Ma, E. H. Hauge, R. B. Weisman and R. E. Smalley, *Science*, 2002, **297**, 593–596.
- (a) M. Endo, M. S. Strano and P. M. Ajayan, Carbon Nanotubes, *Top. Appl. Phys.*, 2008, **111**, 13–61; (b) J. Robertson, *Mater. Today*, 2007, **10**(1–2), 36–43; (c) A. Bianco, K. Kostarelos, C. D. Partidos and M. Prato, *Chem. Commun.*, 2005, 571–577.
- (a) C. Dekker, *Phys. Today*, 1999, **52**(5), 22–28; (b) R. Saito, M. Fujita, G. Dresselhaus and M. S. Dresselhaus, *Appl. Phys. Lett.*, 1992, **60**, 2204–2206.
- R. Saito, G. Dresselhaus and M. S. Dresselhaus, *Phys. Rev. B*, 2000, **61**, 2981–2990.
- X. Sun, S. Zaric, D. Daranciang, K. Welsher, Y. Lu, X. Li and H. Dai, *J. Am. Chem. Soc.*, 2008, **130**, 6551–6555.
- S. M. Bachilo, M. S. Strano, C. Kittrell, R. H. Hauge, R. E. Smalley and R. B. Weisman, *Science*, 2002, **298**, 2361–2366.
- (a) A. M. Rao, P. C. Eklund, S. Bandow, A. Thess and R. E. Smalley, *Nature*, 1997, **388**, 257–259; (b) S. Kazaoui, N. Minami, R. Jacquemin, H. Kataura and Y. Achiba, *Phys. Rev. B*, 1999, **60**, 13339–13342; (c) P. Petit, C. Mathis, C. Journet and P. Bernier, *Chem. Phys. Lett.*, 1999, **305**, 370–374.
- J. E. Fischer, *Acc. Chem. Res.*, 2002, **35**, 1079–1086.
- E. Jouguelet, C. Mathis and P. Petit, *Chem. Phys. Lett.*, 2000, **318**, 561–564.
- (a) S. Kazaoui, N. Minami, H. Kataura and Y. Achiba, *Synth. Met.*, 2001, **121**, 1201–1202; (b) M. J. O'Connell, E. E. Eibergen and S. K. Doorn, *Nat. Mater.*, 2005, **4**, 412–418.
- M. Zheng and B. A. Diner, *J. Am. Chem. Soc.*, 2004, **126**, 15490–15494.
- T. J. McDonald, D. Svedruzic, Y.-H. Kim, J. L. Blackburn, S. B. Zhang, P. W. King and M. J. Heben, *Nano Lett.*, 2007, **7**, 3528–3534.
- L. Kavan and L. Dunsch, *ChemPhysChem*, 2007, **8**, 974–998.
- (a) K.-i. Okazaki, Y. Nakato and K. Murakoshi, *Phys. Rev. B*, 2003, **68**, 035434; (b) K. Murakoshi and K.-i. Okazaki, *Electrochim. Acta*, 2005, **50**, 3069–3075.
- R. L. McCreery, *Electrochemical Properties of Carbon Surfaces*, Dekker, New York, 1999, p. 631.

- 25 (a) A. J. Downard, *Electroanalysis*, 2000, **12**, 1085–1096; (b) J. Pinson and F. Podvorica, *Chem. Soc. Rev.*, 2005, **34**, 429–439.
- 26 See for instance: K. Gong, Y. Yan, M. Zhang, L. Su, S. Xiong and L. Mao, *Anal. Sci.*, 2005, **21**, 1383–1393.
- 27 I. Heller, J. Kong, H. A. Heering, K. A. Williams, S. G. Lemay and C. Dekker, *Nano Lett.*, 2005, **5**, 137–142.
- 28 I. Heller, J. Kong, K. A. Williams, C. Dekker and S. G. Lemay, *J. Am. Chem. Soc.*, 2006, **128**, 7353–7359.
- 29 (a) P. Kim, T. W. Odom, J.-L. Huang and C. M. Lieber, *Phys. Rev. Lett.*, 1999, **82**, 1225–1228; (b) M. Ouyang, J.-L. Huang and C. M. Lieber, *Annu. Rev. Phys. Chem.*, 2002, **53**, 201–220; (c) Y.-K. Kwon, S. Saito and D. Tomanek, *Phys. Rev. B*, 1998, **58**, 13314–13317.
- 30 M. Melle-Franco, M. Marcaccio, D. Paolucci, F. Paolucci, V. Georgakilas, D. M. Guldi, M. Prato and F. Zerbetto, *J. Am. Chem. Soc.*, 2004, **126**, 1646–1647.
- 31 A. M. Becka and C. J. Miller, *J. Phys. Chem.*, 1992, **96**, 2657–2668.
- 32 M. Ouyang, J.-L. Huang and C. M. Lieber, *Acc. Chem. Res.*, 2002, **35**, 1018–1025.
- 33 S. Reich, J. Maultzsch, C. Thomsen and P. Ordejón, *Phys. Rev. B*, 2002, **66**, 035412.
- 34 A. Kukovecz, Ch. Kramberger, V. Georgakilas, M. Prato and H. Kuzmany, *Eur. Phys. J. B*, 2002, **28**, 223–230.
- 35 D. Paolucci, M. Melle-Franco, M. Iurlo, M. Marcaccio, M. Prato, F. Zerbetto, A. Pénicaud and F. Paolucci, *J. Am. Chem. Soc.*, 2008, **130**, 7393–7399.
- 36 A. J. Bard and L. R. Faulkner, *Electrochemical Methods: Fundamentals, and Applications*, Wiley, New York, 2001, ch. 17.
- 37 R. B. Weisman and S. M. Bachilo, *Nano Lett.*, 2003, **3**, 1235–1238.
- 38 G. D. Scholes and G. Rumbles, *Nat. Mater.*, 2006, **5**, 683–696.
- 39 (a) A. Callegari, S. Cosnier, M. Marcaccio, D. Paolucci, F. Paolucci, V. Georgakilas, N. Tagmatarchis, E. Vazquez and M. Prato, *J. Mater. Chem.*, 2004, **14**, 807–810; (b) A. Callegari, M. Marcaccio, D. Paolucci, F. Paolucci, N. Tagmatarchis, D. Tasis, E. Vazquez and M. Prato, *Chem. Commun.*, 2003, 2576–2577.
- 40 D. M. Guldi, G. M. A. Rahman, V. Sgobba and C. Ehli, *Chem. Soc. Rev.*, 2006, **35**, 471–487.
- 41 D. M. Guldi, *J. Phys. Chem. B*, 2005, **109**, 11432–11441.
- 42 V. Sgobba and D. M. Guldi, *J. Mater. Chem.*, 2008, **18**, 153–157.
- 43 D. M. Guldi, M. Marcaccio, D. Paolucci, F. Paolucci, N. Tagmatarchis, D. Tasis, E. Vazquez and M. Prato, *Angew. Chem., Int. Ed.*, 2003, **42**, 4206–4209.
- 44 See for instance: (a) D. M. Guldi, G. N. A. Rahman, J. Ramey, M. Marcaccio, D. Paolucci, F. Paolucci, S. H. Qin, W. T. Ford, D. Balbinot, N. Jux, N. Tagmatarchis and M. Prato, *Chem. Commun.*, 2004, 2034–2035; (b) D. M. Guldi, G. N. A. Rahman, N. Jux, N. Tagmatarchis and M. Prato, *Angew. Chem., Int. Ed.*, 2004, **43**, 5526–5530; (c) M. Alvaro, P. Atienzar, P. de la Cruz, J. L. Delgado, H. Garcia and F. Langa, *J. Phys. Chem. B*, 2004, **108**, 12691–12697; (d) L. Sheeney-Hai-ichia, B. Basnar and I. Willner, *Angew. Chem., Int. Ed.*, 2005, **44**, 78–83; (e) D. M. Guldi, H. Taieb, G. N. A. Rahman, N. Tagmatarchis and M. Prato, *Adv. Mater.*, 2005, **17**, 871–875; (f) C. Ehli, G. M. A. Rahman, N. Jux, D. Balbinot, D. M. Guldi, F. Paolucci, M. Marcaccio, D. Paolucci, M. Melle-Franco, F. Zerbetto, S. Campidelli and M. Prato, *J. Am. Chem. Soc.*, 2006, **128**, 11222–11231; (g) D. M. Guldi, G. N. A. Rahman, S. Qin, M. Tchoul, W. T. Ford, M. Marcaccio, D. Paolucci, F. Paolucci, S. Campidelli and M. Prato, *Chem.–Eur. J.*, 2006, **12**, 2152–2161; (h) D. M. Guldi, G. N. A. Rahman, J. Ramey, M. Marcaccio, D. Paolucci, F. Paolucci, S. Qin, W. T. Ford, D. Balbinot, N. Jux, N. Tagmatarchis and M. Prato, *Chem. Commun.*, 2004, 2034–2035; (i) N. Martiín, L. Sánchez, M. A. Herranz, B. Illescas and D. M. Guldi, *Acc. Chem. Res.*, 2007, **40**, 1015–1024; (j) M. Á. Herranz, N. Martín, S. Campidelli, M. Prato, G. Brehm and D. M. Guldi, *Angew. Chem., Int. Ed.*, 2006, **45**, 4478–4482; (k) M. Á. Herranz, C. Ehli, S. Campidelli, M. Gutiérrez, G. L. Hug, K. Ohkubo, S. Fukuzumi, M. Prato, N. Martín and D. M. Guldi, *J. Am. Chem. Soc.*, 2008, **130**, 66–73.
- 45 (a) T. A. Felekis and N. Tagmatarchis, *Rev. Adv. Mater. Sci.*, 2005, **10**, 272–276; (b) M. Terrones, A. G. Souza and A. M. Rao, Carbon Nanotubes, *Top. Appl. Phys.*, 2008, **111**, 531–566.
- 46 (a) Q. Xie, F. Arias and L. Echegoyen, *J. Am. Chem. Soc.*, 1993, **115**, 9818–9819; (b) C. A. Reed, K.-C. Kim, R. D. Bolskar and L. J. Mueller, *Science*, 2000, **289**, 101–104; (c) C. Bruno, I. Doubitski, M. Marcaccio, F. Paolucci, D. Paolucci and A. Zaopo, *J. Am. Chem. Soc.*, 2003, **125**, 15738–15739.
- 47 D. M. Guldi, E. Menna, M. Maggini, M. Marcaccio, D. Paolucci, F. Paolucci, S. Campidelli, M. Prato, G. M. A. Rahman and S. Schergna, *Chem.–Eur. J.*, 2006, **12**, 3975–3983.
- 48 F. D'Souza, R. Chitta, A. S. D. Sandanayaka, N. K. Subbaiyan, L. D'Souza, Y. Araki and I. Osamu, *J. Am. Chem. Soc.*, 2007, **129**, 15865–15871.
- 49 C. Cioffi, S. Campidelli, C. Soambar, M. Marcaccio, G. Marcolongo, M. Meneghetti, D. Paolucci, F. Paolucci, C. Ehli, G. M. A. Rahman, V. Sgobba, D. M. Guldi and M. Prato, *J. Am. Chem. Soc.*, 2007, **129**, 3938–3945.
- 50 G. Rotas, A. S. D. Sandanayaka, N. Tagmatarchis, T. Ichihashi, M. Yudasaka, S. Iijima and O. Ito, *J. Am. Chem. Soc.*, 2008, 4725–4731.
- 51 M. I. Katsnelson, *Mater. Today*, 2007, **10**(1–2), 20–27.
- 52 (a) D. Guldi, N. Martín and M. Pratoeds (eds.), *J. Mater. Chem.*, 2008, **18**, 1401–1604 (theme issue: carbon nanostructures); (b) *Fullerenes, Principles and Applications*, ed. F. Langa and J.-F. Nierengarten, Royal Society of Chemistry, Cambridge, UK, 2007; (c) M. Nanjo, P. W. Cyr, K. Liu, E. H. Sargent and I. Manners, *Adv. Funct. Mater.*, 2008, **18**, 470–477; (d) R. Bakry, R. M. Vallant, M. Najam-Ul-Haq, M. Rainer, Z. Szabo, C. W. Huck and G. K. Bonn, *Int. J. Nanomed.*, 2007, **2**, 639–649; (e) C. Yang, J. Y. Kim, S. Cho, J. K. Lee, A. J. Heeger and Fred Wudl, *J. Am. Chem. Soc.*, 2008, **130**, 6444–6450; (f) C. Bruno, M. Marcaccio, D. Paolucci, C. Castellarin-Cudia, A. Goldoni, A. V. Streletski, T. Drewello, S. Barison, A. Venturini, F. Zerbetto and F. Paolucci, *J. Am. Chem. Soc.*, 2008, **130**, 3788–3796.
- 53 A. K. Geim and K. S. Novoselov, *Nat. Mater.*, 2007, **6**, 183–191.